TECHNICAL REPORT
NATICK/TR-92/013

AD _____

STRUCTURAL AND VIBRATIONAL ANALYSIS OF A PLASTIC ANNULAR WIND TUNNEL PARACHUTE MODEL

By
Richard J. Benney

December 1991

FINAL REPORT
May 1991 - September 1991

APPROVED FOR PUBLIC RELEASE;
DISTRIBUTION UNLIMITED

UNITED STATES ARMY NATICK
RESEARCH, DEVELOPMENT AND ENGINEERING CENTER
NATICK, MASSACHUSETTS 01760-5000

AERO-MECHANICAL ENGINEERING DIRECTORATE

REPORT DOCUMENTATION PAGE

Form Approved
OMB No. 0704-0188

1. AGENCY USE ONLY (Leave blank)	2. REPORT DATE	3. REPORT TYPE AND DATES COVERED
	December 1991	Final Report May 91 to Sep 91

4. TITLE AND SUBTITLE

STRUCTURAL AND VIBRATIONAL ANALYSIS OF A PLASTIC ANNULAR WIND TUNNEL PARACHUTE MODEL

5. FUNDING NUMBERS

PE 62786D
PR 1L162786D283
TA AJ
WU HOO

6. AUTHOR(S)

RICHARD JOHN BENNEY

7. PERFORMING ORGANIZATION NAME(S) AND ADDRESS(ES)

U.S. Army Natick RD&E Center
ATTN: STRNC-AC
Natick, MA 01760-5015

8. PERFORMING ORGANIZATION REPORT NUMBER

NATICK/TR-91/013

9. SPONSORING/MONITORING AGENCY NAME(S) AND ADDRESS(ES)

10. SPONSORING/MONITORING AGENCY REPORT NUMBER

11. SUPPLEMENTARY NOTES

12a. DISTRIBUTION/AVAILABILITY STATEMENT

Approved for public release; distribution unlimited

12b. DISTRIBUTION CODE

13. ABSTRACT (Maximum 200 words)

A plastic annular parachute model will be tested in the U.S. Army Aviation Systems Command Aeroflightdynamics Directorate (AVSCOM/AFDD) wind tunnel at the NASA Ames Research Center in Moffett Field, California. The data from the wind tunnel test will be used to verify results obtained from the computational fluid dynamics program SALE "Simplified Arbitrary Lagrangian-Eulerian" (which is currently being modified by the Engineering Technology Division (ETD) of the Aero-Mechanical Engineering Directorate (AMED) at Natick to improve the prediction of flow fields around parachutes). In this report the parachute model test setup is analyzed to determine the possibility of failure during the wind tunnel test. The model is analyzed in stages of increasing complexity. For each stage the expected deformation and stresses in the model during the wind tunnel test are determined. The eigenvalues, eigenmodes and buckling possibilities at various stages of the analysis are also examined. Most of the stages of the analysis were carried out using the NISA "Numerically Integrated Elements for system analysis" finite element code. The culmination of the analysis is a comparison of various NISA elements. The calculated stresses for the model were well below the yield strength of the model material. The analysis of the model uncovered no structural difficulties for the planned wind tunnel tests.

14. SUBJECT TERMS	15. NUMBER OF PAGES
FLOW FIELDS COMPUTATIONAL FLUID DYNAMICS (CFD) PARACHUTE MODELS PARACHUTES VIBRATIONAL ANALYSIS WIND TUNNEL TESTS YIELD STRENGTH STRUCTURAL ANALYSIS FLUID DYNAMICS ANNULAR PARACHUTES	37
	16. PRICE CODE

17. SECURITY CLASSIFICATION OF REPORT	18. SECURITY CLASSIFICATION OF THIS PAGE	19. SECURITY CLASSIFICATION OF ABSTRACT	20. LIMITATION OF ABSTRACT
UNCLASSIFIED	UNCLASSIFIED	UNCLASSIFIED	SAR

CONTENTS

FIGURES

TABLES

PREFACE

The work described in this report on the Structural and Vibrational Analysis of a Plastic Annular Wind Tunnel Parachute Model was undertaken during the period May 1991 to September 1991. The funding was Program Element 62786D, Project No. 1L162786D283, Task No. AJ, and Work Unit Accession No. HOO. This work was performed by the Engineering Technology Division (ETD) of the Aero-Mechanical Engineering Directorate (AMED).

The author wishes to express his appreciation to Mr. Keith Stein of ETD for his help in this effort.

LIST OF SYMBOLS

D	Flexural Rigidity or Diameter
E	Modulus of Elasticity
I	Moment of Inertia
L	Length of Beam
P	Applied Pressure or Axial Load
r	Radial Distance on Plate
t	Plate Thickness
w	Plate Deflection
ν	Poisson's Ratio
σ_r	Radial Stress in Plate
σ_θ	Tangential Stress in Plate
ω	Natural Frequency
ϱ	Density

STRUCTURAL AND VIBRATIONAL ANALYSIS OF A PLASTIC ANNULAR WIND TUNNEL PARACHUTE MODEL

INTRODUCTION

A plastic annular parachute model will be tested in the U.S. Army Aviation Systems Command Aeroflightdynamics Directorate (AVSCOM/AFDD) wind tunnel at NASA Ames Research Center in Moffett Field, California. AFDD has a closed circuit, single return, continuous flow wind tunnel. The wind tunnel test section consists of a 7-by 10-foot test area which is 15 feet long. The air speed of the tunnel can be varied from 0 to 380 ft/s. The plastic parachute model testing will be conducted at various speeds up to a maximum of 150 ft/s. The wind tunnel test results will be compared to the flow characteristics that have been predicted from the mathematical model using the Computational Fluid Dynamics (CFD) code "SALE" (Simplified Arbitrary Lagrangian-Eulerian). SALE is being modified by the Engineering Technology Division (ETD) of the Aero-Mechanical Engineering Directorate (AMED) at Natick to predict flow fields around parachutes (ref. 1). The wind tunnel test will determine the experimental pressure field on and around the parachute model, along with the velocity field and the drag. The test results will provide a measure of the accuracy of the SALE code at this stage of its modifications.

The rigid plastic parachute model is used instead of a flexible fabric model to simplify the test set up and allow for downstream supports which are discussed further below. The plastic parachute model was fabricated from Acrylonitrile Butadiene-Styrene (A.B.S.) and is axisymmetric in geometry to the flow direction. The model dimensions and material properties are given in Figure 1. The model test set up (Figure 2) was analyzed to predict the response of the model system during the wind tunnel test. The test set up consists of three "beam" supports attached at one end to the rigid parachute model. The farthest downstream end of each beam is attached to a load cell which is mounted to a strut in the center of the tunnel test section. These "downstream" supports are used to minimize the distortion of the flow field around the parachute model and therefore more closely represent the model used in SALE.

While the downstream supports may introduce an instability to the model, minimizing the obstruction of the flow field upstream from the model is considered critical for this wind tunnel test. Upstream supports would of course provide stability. However, they would also disturb the incoming flow field. Seven pressure sensors

are attached to the model along a meridional line. The pressure sensors were inserted into predrilled holes on the model and epoxied into position. The sensors have the same thickness as the model in order to minimize the disturbance to the flow. The required wires for the sensors were epoxied into small grooves that were cut out of the model. The wires surface at the beam supports and follow the beams downstream to the test stand. The analysis of the final design does not incorporate the pressure sensor attachments or the wire grooves. The parachute shell is considered to be a homogeneous, isotropic structure. The three beams used for the downstream support are considered to be simple Euler beams. The ultimate goal of the analysis is to confirm that the plastic parachute model with the three beam support will withstand the loading caused by the wind tunnel.

Analysis

The analysis of the plastic parachute model was performed in stages of increasing complexity. Each stage is a more accurate representation of the model and provided the author increased confidence in the results. The pressure distribution on the model during the wind tunnel test was predicted using SALE, and the maximum pressure was found to be approximately 0.27 psi. The pressure distribution considered for the various models is taken as a constant 0.5 psi to represent a "worst case" pressure. A brief description of each of the major stages taken during the analysis is listed below.

- The problem was first modelled by considering a flat circular plate which was determined to represent a worst case for deflection. The flat circular plate has a clamped inside diameter and a free outside diameter with a constant "worst case" pressure applied on one face. The exact solution from simple plate theory was determined. The solution was also determined with the finite element package NISA "Numerically Integrated Elements for System Analysis" (ref. 2) using axisymmetric solid elements. This was the first time NISA had been used by the author. The results of the two analyses are compared.

- The second model considered is an axisymmetric model with boundary conditions which restrict axial deflection of the farthest downstream location on the model. A constant "worst case" pressure is applied on the inside surface of the shell structure. Five separate NISA runs were made using different NISA elements and the results compared.

- The third model considered incorporates the axisymmetric shell but has nonaxisymmetric boundary conditions. Three of the farthest downstream nodal points located at 120 degree intervals around the axis of symmetry are constrained in the flow direction. A constant "worst case" pressure is applied on the inside surface of the shell structure. Two runs are made with different NISA elements and the results compared.

- The fourth model considered is the final design for the wind tunnel test. The axisymmetric shell is coupled with nonaxisymmetric boundary conditions. The shell is supported by three 3/8 inch diameter beams. The beams are attached to the shell at one end as described in the above case. The other ends are attached to a "sting" (supplied by ETD) which incorporates the load cell (supplied by AFDD). The sting is considered to be a rigid support. The beams are fixed to the sting at 120 degree intervals at a radial distance of 3/4 inch from the axis of symmetry. Two sets of beams have been fabricated for the wind tunnel test. The "long beams" have an assembled length of 20 inches and the "short beams" length is 15 inches. Both models are run using NISA and the results tabulated.

As the above short descriptions indicate, a number of different NISA elements and element combinations were used for the analysis. The multiple runs on NISA served many purposes including a build up in confidence of the finite element results, a comparison of different NISA elements and an introduction to NISA and its capabilities. The remainder of this report details the progression of the analysis of the physical model.

FLAT CIRCULAR PLATE MODEL

The first model used to find an upper bound for the deflections of the plastic annular parachute was a flat circular plate. This plate model represents a worst case for deflection because the actual model would be considerably stiffer due to its shell type structure. The analysis of this simplified model of the parachute also served as an introduction to two of the NISA capabilities which are used throughout the rest of the analysis (1. static analysis to determine deflections, stresses, and strains and 2. eigenvalue analysis to determine natural frequencies and mode shapes). A 0.25 inch thick plate with an inside radius of 5 inches and an outside radius of 10 inches was analyzed. The plate is clamped around its inside diameter, free around its outside diameter and has a constant pressure of 0.5 psi applied along the top surface. The pressure applied is a worst case pressure based on the prediction from SALE and checked by a simple analysis of the drag expected on the model at the wind tunnel test air speed (150ft/s). The governing differential equation (ref. 3) for the plate with this symmetric loading is

$$\frac{1}{r}\frac{d}{dr}\left\{r\frac{d}{dr}\left[\frac{1}{r}\frac{d}{dr}\left(r\frac{dw}{dr}\right)\right]\right\}=\frac{P}{D} \quad , \tag{1}$$

$$\text{where} \qquad D=\frac{Et^3}{12(1-\nu^2)} \quad . \tag{2}$$

The four boundary conditions for the plate, two at the inside diameter and two at the outside diameter, are

$$w\Big|_{r=5}=0 \quad , \quad \frac{dw}{dr}\Big|_{r=5}=0 \quad ,$$

$$\left[\frac{d^2w}{dr^2}+\frac{\nu}{r}\frac{dw}{dr}\right]\Big|_{r=10}=0 \quad , \quad \frac{d}{dr}\left[\frac{1}{r}\frac{d}{dr}\left(r\frac{dw}{dr}\right)\right]\Big|_{r=10}=0 \quad . \tag{3}$$

The solution to the governing differential equation with these boundary conditions and the parameters listed in Figure 1 is

$$w(r)=P[\frac{r^4}{2747.3}-0.291r^2\ln r-11.43\ln r+0.825r^2+9.26]\ . \qquad (4)$$

The maximum calculated deflection of the centerline of the plate is 0.3 inches at the plate's outside diameter. As discussed above, this deflection represents a worst case for the actual model. The stresses in the plate were also calculated and are

$$\sigma_r(r)=P[-20.16r^2+3120\ln r-\frac{32928}{r^2}-4876.8] \qquad (5)$$

and

$$\sigma_\theta(r)=P[-11.52r^2+3120\ln r+\frac{32928}{r^2}-6556.8]\ . \qquad (6)$$

The plate model was also analyzed using NISA. The NISA model consisted of eight axisymmetric solid elements (NISA element NKTP=3). The node and element numbering are shown in Figure 3. This node and element configuration was used because it has already been generated in a sample problem supplied with the NISA software. The maximum plate deflections, radial stresses and the first three mode shapes predicted by NISA are shown in Figures 4,5 and 6, respectively. Note that all of these figures represent a cross section of the plate from r=5 to r=10 inches. The mode shapes in Figure 6 are as expected for the boundary conditions given by equation 3 and the axisymmetric elements used. Table 1 below summarizes the results of the analysis from theory and NISA.

The values of the first two natural frequencies predicted from theory were obtained from reference 4. The values calculated from theory are determined in ref. 4 by assuming a harmonic solution for the governing differential plate equations including inertia terms. This technique separates the time and space variables. Next, a Fourier series solution is assumed to yield a set of differential equations in terms of the Fourier coefficients. This eliminates the theta dependence. The solution of these equations is in the form of Bessel functions. The frequencies are determined by setting up the appropriate equations in terms of the Bessel function solutions and finding the roots of the equation generated by setting the determinant equal to zero. The eigenvalues were calculated by NISA using the "conventional subspace iteration method." This algorithm (the simplest of four available methods in NISA) uses "simultaneous inverse iterations with a set of vectors until the eigenvalues" have reached a given tolerance. A "lumped mass" formulation technique was used for all NISA runs.

TABLE 1 Theory vs. NISA Results for Flat Plate Model

TYPE OF ANALYSIS	THEORY	NISA
DEFLECTION AT r=10 (inches)	0.3006	0.2929
$\sigma_r(5)$ at top surface (psi)	834	827
ω_1 first natural frequency (HZ)	51.9	52.3
ω_2 second natural frequency (HZ)	338	335
ω_3 third natural frequency (HZ)	---	936

The results between NISA and theory are in very close agreement, especially when considering the coarse finite element mesh that was used. These results provide confidence in the NISA computer code. The maximum predicted stresses are also well below the yield strength of the model material ($\sigma_{y\ ABS}$=2,400psi).

AXISYMMETRIC MODEL USING NISA

The plastic parachute model was analyzed at this stage of the analysis as an axisymmetric solid with axisymmetric loading of 0.5 psi pressure acting along the inside surface of the model. The boundary condition used for this analysis is the vanishing of axial deflection at the nodes on the model that are located farthest downstream (positive y-axis). Five different cases were run using four different NISA element types. The first three cases consisted of axisymmetric elements for which the above boundary conditions are sufficient. The last two cases used thin and general shell elements, respectively, and required added constraints to restrict rigid body motion in the y=constant plane. These added constraints are described later. The final design for the test setup had not been confirmed at this point in the analysis. Therefore various node/element layouts were constructed of the parachute shell structure which could be reused later with the final test setup boundary conditions. These layouts were run and the results compared for the present boundary conditions. The node points for the first two cases were generated from the same Fortran program (written by Keith Stein) used to generate nodes for the SALE program. The Fortran program generates coordinates of points located on the parachute model which is a portion of an ellipse. A short description of each case is given below. A summary of all five cases and the results of each case are located in Table 2.

TABLE 2 Axisymmetric Model with Axisymmetric Boundary Conditions

CASE #	DESCRIPTION OF ELEMENT
1	Axisymmetric Shell Elements
2	Axisymmetric Shell Elements
3	Axisymmetric Solid Elements
4	Thin Shell Elements
5	3-D General Shell Element

CASE #	1	2	3	4	5
NKTP=	36	36	3	40	20
# of Elements	16	50	100	384	384
# of Nodes/Elem	2	2	4	4	4
DOF/Node	3	3	2	6	6
Max UX (inches) Node #	0.00343 9	0.00346 26	-0.00369 112	0.00334 9	-0.00338 213
Max UY (inches) Node #	0.0174 9	0.0195 26	0.0171 29	0.0166 213	0.017 213
Prin. Stress 1 psi /Node #	35.86 9	37.75 26	63.0 120	36.19 298	36.64 230
Prin. Stress 3 psi /Node #	-37.05 4	-43.68 9	-84.5 18	-39.4 259	-40.54 225
ω_1 Hz	92.17	89.84	101.7	38.84	37.58
ω_2 Hz	302.4	315.5	481.8	39.1	37.76
ω_3 Hz	363.6	374.4	547.3	68.01	66.89
ω_4 Hz	---	---	---	68.01	66.89
ω_5 Hz	---	---	---	75.54	72.2
ω_6 Hz	---	---	---	75.54	72.2
ω_7 Hz	---	---	---	101.5★	101.0★

★ First Axisymmetric Mode

CASE # 1 and 2

The first two cases used "axisymmetric shell elements" (NKTP=36). Case # 1 consisted of 17 nodes (16 elements). The 17 nodes were generated by the default output of the Fortran program mentioned above. Case # 2 consisted of 51 nodes (50 elements). These nodes were generated by a simple modification of the above mentioned Fortran program. Figure 7 shows the node layout for Case # 1. Figure 8 is a superposition of the undeformed and deformed shapes. The layout for Case # 2 is similar.

CASE # 3

The third case uses "axisymmetric solid elements" (NKTP=3). The model has 153 nodes (100 elements). Figure 9 shows a portion of the element and nodal point numbering. The nodes for this case were generated from a Fortran program which used the nodes of Case # 2 as input. The nodes from Case # 2 were used as the middle surface nodes of the model and the program generated the inside and outside surface nodes needed for the elements used in this case. The Fortran program used a simple finite difference approximation to determine the normal direction at each middle surface node and then generated inside and outside surface nodal coordinates by adding half the shell thickness in each direction. Figure 10 is a superposition of the undeformed and deformed geometry for this case.

CASE # 4 and # 5

These cases use the "thin shell elements" (NKTP=40) and the "3-D general shell elements" (NKTP=20), respectively. The difference between these two elements is that the general shell elements include the effect of transverse shear while the thin shell elements do not. The finite element mesh is the same for both cases. The model is made up of 408 nodes (384 elements). The node point coordinates were generated in a Fortran program which used the coordinates of the nodes from Case # 1 as input. The program generates nodal coordinates at fifteen degree intervals about the axis of symmetry (y axis). A view of a portion of the element/node configuration is shown in Figure 11. The boundary conditions for these cases had to be modified to eliminate rigid body translation. This was accomplished by restricting "z" direction translation for two nodes located on the x-axis and restricting "x" direction translation for two nodes located on the z-axis. Figure 12 shows the resultant deflections of the model for Case # 4. The figures for Case # 5 are virtually identical to Case # 4, as can be seen by examination of the results in Table 2. Also, notice (Table 2) that these cases have six degrees of freedom (DOF) at each node so that the first axisymmetric mode shape doesn't appear until mode number seven. The actual mode shapes are not shown for these models but were visualized by the author while running NISA. The value of ω_1 for Cases 1,2, and 3 in Table 2 are reasonably close to the values of ω_7 for Cases 4 and 5. The lower mode shapes for Cases 4 and 5 include twisting and bulging about planes of symmetry.

SUMMARY OF AXISYMMETRIC MODEL

The results of the five cases are very close (see Table 2). The coordinates of the node numbers given along with the maximum deflections and stresses are close to each other for all five cases except Case # 3. The difference is due to the different elements used. The third case has node points on both inside, middle, and outside surfaces of the shell. The nodal principal stresses are greater in magnitude on the inside and outside surfaces. The values

for the principal stresses on the middle surface are much closer to the values given for the other cases. Note also that the natural frequencies for Case # 3 are much higher than for Cases 1 and 2. This is because the elements used in Case # 3 have only two DOF (versus three DOF for Case 1 and 2) which significantly affects the eigenvalue analysis. Any of these cases would be adequate to represent the model if the boundary conditions were to remain axisymmetric. In the perfect model the pressure distribution produced by the flow field will be axisymmetric. However, during actual testing, there will be disturbances which will cause perturbations in the flow field. Therefore the fourth and fifth case represent the plastic parachute model more accurately than Cases 1,2, and 3. Vortex shedding will be present during the test and the ability to excite the first six modes of Cases 4 and 5 are possible. The first three cases can not predict these modes.

AXISYMMETRIC SHELL WITH NONAXISYMMETRIC BOUNDARY CONDITIONS

The best information available at this time indicates that the actual plastic parachute test model will be supported at three points. These points will be located at 120 degree intervals, at the same radial distance, and at the farthest downstream axial distance on the shell. These points are shown in Figures 13 through 16 as small black circles on the restricted nodes. These figures will be discussed further below. The deflections for this model are expected to be greater than the results in the last five cases but still less than the flat circular plate deflections. The axisymmetric elements of Cases 1,2 and 3 above are unable to include this type of support boundary condition. Therefore only the "thin shell elements" and "3-D general shell elements" are used to model the parachute shell for this analysis.

The final design of the test setup had not been determined at this time. Therefore, the next step was to be sure that the shell supported at three points would withstand the pressure loading of the wind tunnel test. The boundary conditions for NISA Cases 4 and 5 were changed to model the three point support. The three support points were restricted from deflections in the axial (y axis) direction only. Also, three weak springs were included to restrict the rigid body translation of the shell without inducing any significant stresses. Each of the three restricted nodes has one spring attached to it and the other end of each spring is attached to a fixed point on the y axis. Two other nodes are constrained to restrict rigid body rotation. This was accomplished by restricting two nodes on the x-axis of the shell from motion in the z-direction. This restriction does not affect the static solution because the loading is axisymmetric. However, these restrictions do introduce some unexpected mode shapes. The results of the NISA runs for the two models are listed in Table 3.

TABLE 3 Axisymmetric Shell, Three Point Constraint

NISA ELEMENT TYPE NKTP	40 THIN SHELL	20 3-D GEN.SHELL
MAX RESULTANT DISPLACE-MENT (INCHES) NODE #	0.04216 83	0.0407 83
PRIN. STRESS 1 (mid surface) psi NODE #	260.5 1	259.1 1
PRIN. STRESS 3 (mid surface) psi NODE #	-132.7 276	-127.5 276
ω_1 Hz	0.598	0.598
ω_2 Hz	24.74	23.8
ω_3 Hz	24.97	24.0
ω_4 Hz	50.3	50.0
ω_5 Hz	52.9	52.7
ω_6 Hz	72.75	70.3
ω_7 Hz	74.83	71.4
ω_8 Hz	78.86	78.5
ω_9 Hz	115.9	114.5
ω_{10} Hz	137.6	130.7

The tabulated results show that the principal stresses are well below the yield stress of A.B.S. Therefore the shell portion of the model will not fail under the action of the worst case loading with a three point constraint. The boundary conditions used are equivalent to applying three point loads at the support connection. Figure 13 shows the resultant displacements for the NKTP=40 model. Figures 14,15, and 16 are the three principal stresses in the model along the middle surface (NKTP=40).

The results from NISA around the three restricted nodes is a critical area. The mesh was very coarse and consequently the results near these restricted nodes is not expected to be accurate. Therefore, a simple "handbook" calculation was performed as a rough check on the principal stress near one of the three restricted nodes. The resultant load in the y-direction (calculated by NISA) for each of the three restricted nodes is 34.17 lb. The formula used (ref. 5) yields the principal stress in a spherical cap which is loaded with a constant pressure about a small area with a given radius. The radius was taken as 3/16 inch which corresponds to a support shaft of 3/8 inch diameter. A value of 20 inches was used for the sphere radius which represents a worst case for the model. This calculation yields a maximum principal stress of 875 psi which

is still well below the yield point of A.B.S.

The first ten natural frequencies were calculated using NISA and are also listed in Table 3. Eight of the mode shapes corresponding to these eigenvalues will reappear and be discussed in the next section. Mode numbers one and nine are particular to the set of boundary conditions used for this model. Mode number one is due to the three springs in the model. The model simply oscillates up and down the axis of symmetry (y-axis) due to the three springs which are fixed to the y-axis. Mode number nine is related to the artificial constraints that were added to the model to restrict rigid body rotation about the axis of symmetry. Neither of these mode shapes will be possible in the final model.

FINAL DESIGN OF MODEL WITH THREE BEAM SUPPORT

The model design was finalized through discussions with personnel at AFDD by Keith Stein of ETD. The existing wind tunnel support structures at AMES, including a load cell, were examined. The existing equipment was determined to be well-suited for the proposed test. The loads from the plastic parachute model on the existing support structure at AMES will be well below any of the upper limits of the equipment. AFDD is also equipped with some flow visualization capabilities. Therefore, ETD's only physical requirements for the test are to supply the plastic parachute shell, the three beam supports and a "sting" which fits over the existing load cell at AFDD. ETD will also provide the pressure sensors and some related electronic equipment which is not considered in the present analysis. The "sting" which fits over the load cell is made from a cylindrical piece of steel which has a two inch outside diameter. The sting is considered "fixed" for this analysis. The three beams slide into predrilled holes in the sting. Each beam is held in place by two set screws which thread through the sting. The beams are fixed at a radial distance of 3/4 inch from the y-axis, which runs through the central axis of the cylindrically shaped sting. The diameter and length of the beam supports were chosen after considering buckling possibilities for the beams. A single beam was considered with a compressive load applied in the axial direction. A simple Euler column with one boundary fixed and one pinned was used to model the beam. The equation representing this model is given below.

$$P_{critical} = \frac{\pi^2 EI}{4L^2} \quad where \quad I = \frac{\pi D^4}{64} \tag{7}$$

Optimal beam lengths of 15 inches and 20 inches and a diameter of 3/8 inch were determined for minimal flow obstruction. Having the option of two different beam lengths for the testing is important. The possibility of vortex shedding from the model for a given wind tunnel speed at or around the same rate as the first few eigenmodes

may lead to "noise" in the data being collected. The ability to run the test at these wind speeds with a different set of beam lengths will permit the collection of more usable data. The critical load for a 3/8 inch diameter beam with a length of 20 inches is 180 lb. The largest expected axial force in one beam is between 10 and 20 lb, therefore the model will not fail due to buckling.

Final Design NISA Runs

The final design was analyzed with both the short beams (15 inches) and the long beams (20 inches). The 3-D General Shell Element (NKTP=20) is used to model the plastic shell with the same element mesh used in the previous runs. The beam supports are modelled with the NISA 3-D General Beam Element (NKTP=39). Each beam support is modelled with one element. The elements are fixed to the shell at one end and fixed in space at the other end where the beams are attached to the sting. This model requires no springs or added constraints because the fixed ends of the beams at the sting restrict all rigid body motion. The beam elements are given a circular cross section with a diameter of 3/8 inch. The actual beams will be made of steel and the properties used for the runs are listed below.

Youngs Modulus (Beams) = 30E+06 psi
Density (Beams) = 7.342E-04 $lbfsec^2/in^4$

The results of the runs with the short and long beams are summarized in table 4 below.

Table 4 Final Design Short & Long Beam Supports

TYPE OF ANALYSIS	SHORT BEAMS	LONG BEAMS	SHAKE TEST SHORT/LONG
MAX RESULTANT DISPLACE-MENT (INCHES) NODE #	0.0504 83	0.0516 219	------
PRIN. STRESS1 (top surface) psi NODE #	344.3 1	353.5 1	------
PRIN. STRESS3 (bottom surface) psi NODE #	-505.4 140	-496.2 140	------
ω_1 Hz	9.134	5.92	------
ω_2 Hz	10.79	7.286	8.6 / 6.2
ω_3 Hz	10.79	7.286	8.6 / 6.2
ω_4 Hz	25.48	25.19	------
ω_5 Hz	25.48	25.19	------
ω_6 Hz	58.08	53.5	------

ω_7 Hz	58.08	53.5	------
ω_8 Hz	68.72	68.08	------
ω_9 Hz	71.48	71.48	------
ω_{10} Hz	73.61	73.22	------
ω_{11} Hz	130.7	130.7	------
ω_{12} Hz	130.7	130.7	------

The results for the principal stresses are similar to the results from the last section for most of the shell except near the three support locations. This is because the boundary conditions are different at these supports. The beams are considered fixed to the shell at these three points and the contact area is increased from the previous cases. The principal stresses are well below the yield strength of the A.B.S. plastic. The deformations are larger for these runs compared to the last case because NISA is giving the resultant deflection of each node. The nodes on the plastic shell are experiencing more axial deflection due to the three beam support. Figures of the deformation contours and stress contours are not shown. They are very similar to the contours given in Figures 13-16. The first twelve eigenvalues are also given for each run. The mode shapes for each eigenvalue will be discussed next.

Mode Shapes

The first three mode shapes are shown in Figure 17. These include the expected torsional and cantilever modes due to the presence of the three beam supports. Note that the influence of the beams on each mode shape can be seen by observing the difference in magnitude between the eigenvalues of each run. A "rap test" was conducted by AVSCOM/AFDD and ETD personnel at NASA Ames Research Center to experimentally determine the natural frequencies of the assembled model. Two accelerometers were attached to the model and the model was set in motion by displacing or tapping it at various locations. The cantilever motion was the least damped and the only mode visible to observers. The frequencies are given in Table 4 above. The only other dominant frequency found during the rap tests was in the 42 to 48 hertz range. The corresponding mode shapes were not determined. These frequencies may be related to the support structure to which the model was mounted.

The fourth and fifth mode shapes are shown in Figure 18. This figure and the rest of the mode shape figures are a superposition of the undeformed model and the scaled deformed mode shape of the model. Mode shapes that are similar to each other are not shown separately. The fourth and fifth mode shapes are a double bulging in the plastic shell with the largest amplitudes appearing at the farthest upstream locations on the shell. The fourth mode is shown in the figure. The fifth mode can be visualized by simply rotating

the x,z plane about the y-axis by 45 degrees. These shapes are expected because the plastic shell is considerably stiffer at its downstream end than its upstream end. Also, the fourth and fifth mode shapes are almost identical to the second and third mode shapes of the last section. The slight difference in the magnitude of the eigenvalues is due to the different boundary conditions for each model. Modes six and seven are shown in Figure 19. These involve a twisting in and out of the x,z plane. These modes also appear as modes four and five from the last case. The similarity of the shapes and the similar eigenvalues for these runs show that the three beam support has little effect on these modes. The eighth, ninth and tenth mode shapes are also similar to each other and are shown in Figure 20. They involve a triple bulge in the shell structure. Mode shapes eight and ten bulge radially about the three beam supports. Mode nine can be visualized by rotating the x,z plane by 22.5 degrees about the y-axis. These mode shapes are also viewed in the previous three point boundary condition cases as modes 6,7, and 8, respectively. Mode shapes eleven and twelve are shown in Figure 21. They involve a four-way bulging effect. Mode shape eleven is shown and mode shape twelve can be visualized by rotating the x,z plane by 22.5 degrees about the y-axis. Mode eleven also appears in the previous cases as mode number ten. The eigenvalues for these cases are nearly identical. Higher eigenvalues and the corresponding mode shapes are not expected to significantly affect the wind tunnel test of the plastic parachute model.

CONCLUSIONS

The major purpose of this report was to evaluate the structural and vibrational characteristics of a plastic parachute model which will be stressed during a test at the U.S Army AVSCOM/AFDD wind tunnel at NASA Ames Research Center. The results of the wind tunnel test will be compared to the theoretical results which have been determined by Keith Stein at ETD by modifying the computational fluid dynamics code SALE. The paper examines various models of the plastic parachute. The model is analyzed in stages of increasing complexity which helped lead to the final design. The intermediate steps taken during the analysis towards the final design were carefully checked and compared to each previous step. Each step therefore has yielded a greater confidence in the final results. The parameters used are either real measurements or heavily scaled values to insure a high safety factor for the wind tunnel test.

The analysis of the various models revealed no major problem areas. The largest calculated stress at any step of the analysis is still significantly less than the yield strength of the A.B.S. plastic used to construct the plastic parachute shell. The eigenvalues and mode shape calculations helped to visualize the various types of shapes and deformations that could occur during the test. The major conclusions of this analysis are:

(1) The expected deflections in the model during the wind tunnel test will be insignificant.

(2) The stresses in the model during the test will be well below the yield strength of the model material.

(3) The model supports will not buckle during the test.

(4) The vibrational characteristics of the model may introduce noise in the data but will not cause failure of the model.

(5) The model will not fail during the wind tunnel test.

This document reports research undertaken at the U.S. Army Natick Research, Development and Engineering Center and has been assigned No. NATICK/TR-[illegible] in the series of reports approved for publication.

REFERENCES

1. Stein, Keith "Computations of the Flow Characteristics of Aerodynamic Decelerators using Computational Fluid Dynamics." Proceedings of AIAA 11th Aerodynamic Decelerator Systems Technology Conference. San Diego, CA. April 9-11, 1991.

2. NISA, Engineering Mechanics Research Corporation. P.O. Box 696, Troy, Michigan 48099.

3. Cook, Robert D. and Young, Warren C. "Advanced Mechanics of Materials" Macmillan Publishing Company. N.Y. 1985.

4. Leissa, Arthur W. "Vibration of Plates." Ohio State University, Columbus, Ohio 1969. U.S. Department of Commerce, National Technical Information Service. N70-18461.

5. Roark, Raymond J. "Formulas for Stress and Strain" McGraw-Hill Book Company. 4th ed. N.Y. 1965. (page 304, Case # 20)

APPENDIX

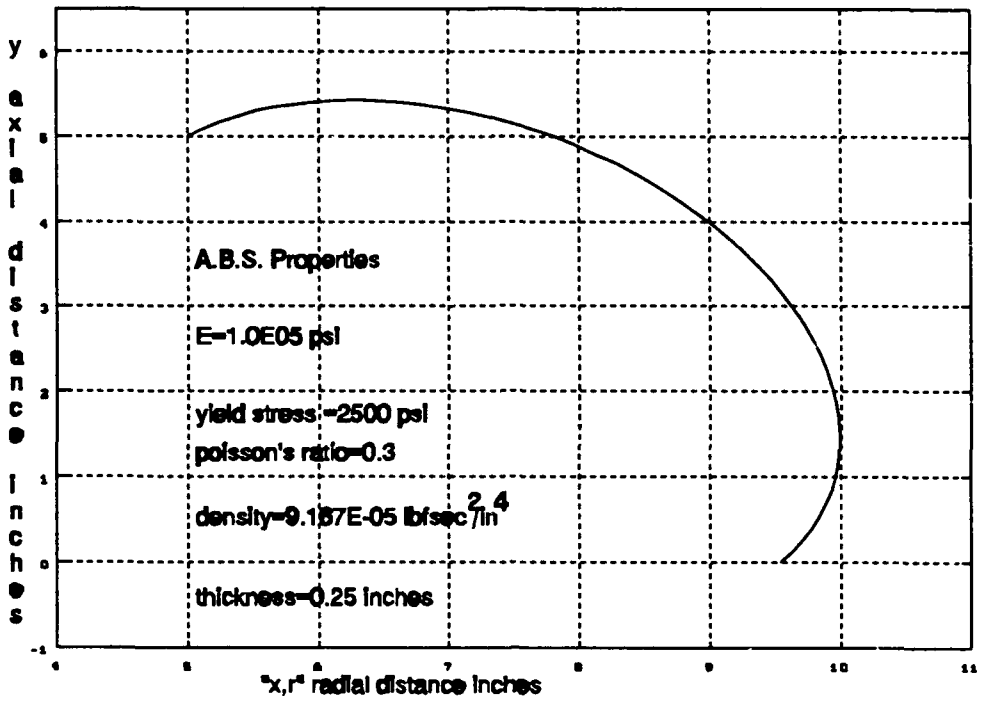

Figure 1. Model Dimensions

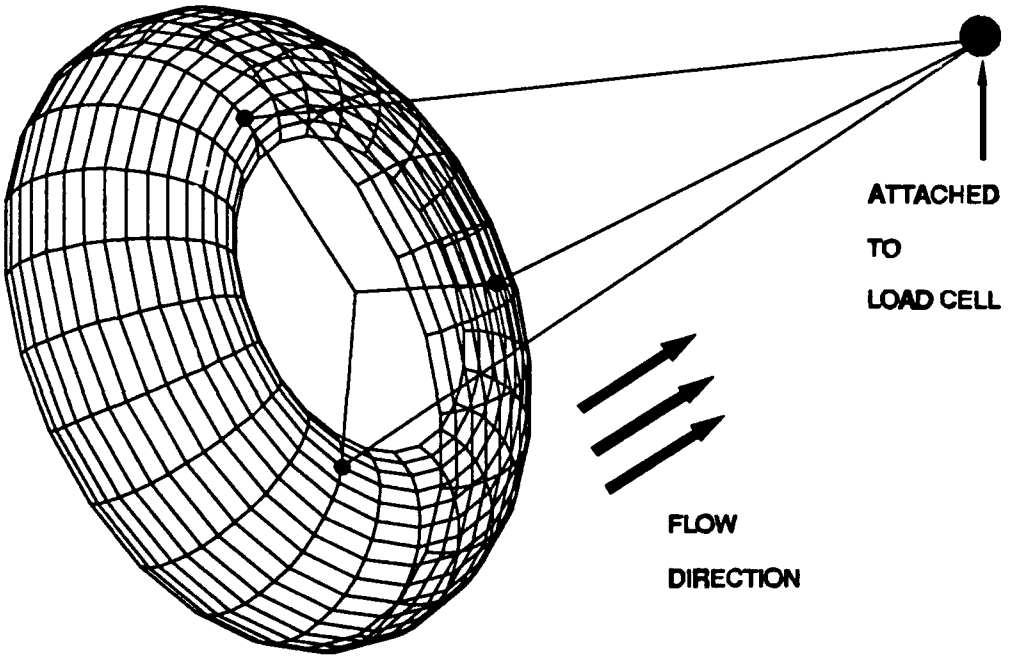

Figure 2. Model Test Set Up

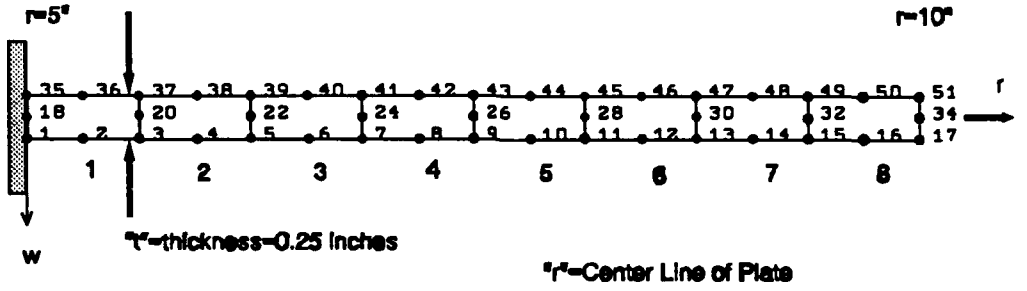

Figure 3. Node and Element Numbering Plate

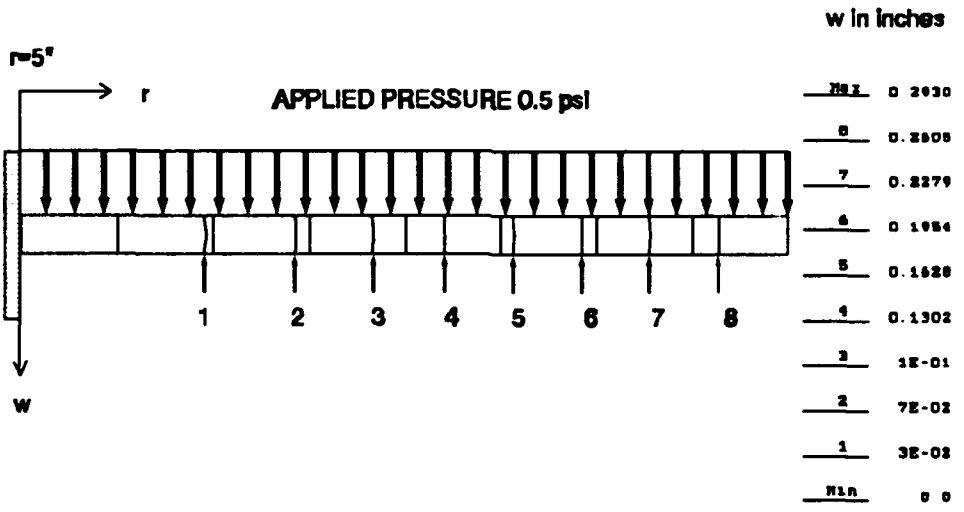

Figure 4. Plate Deflections

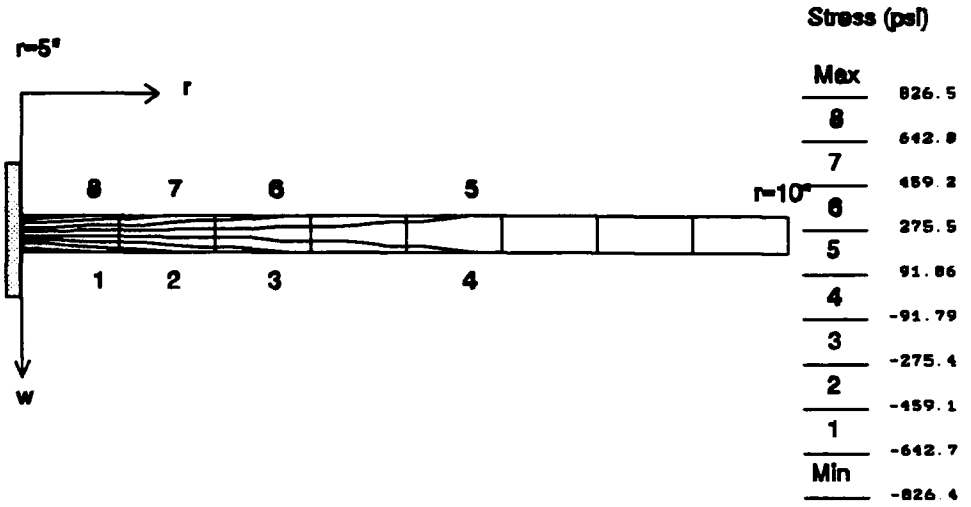

Figure 5. Radial Stresses in Plate

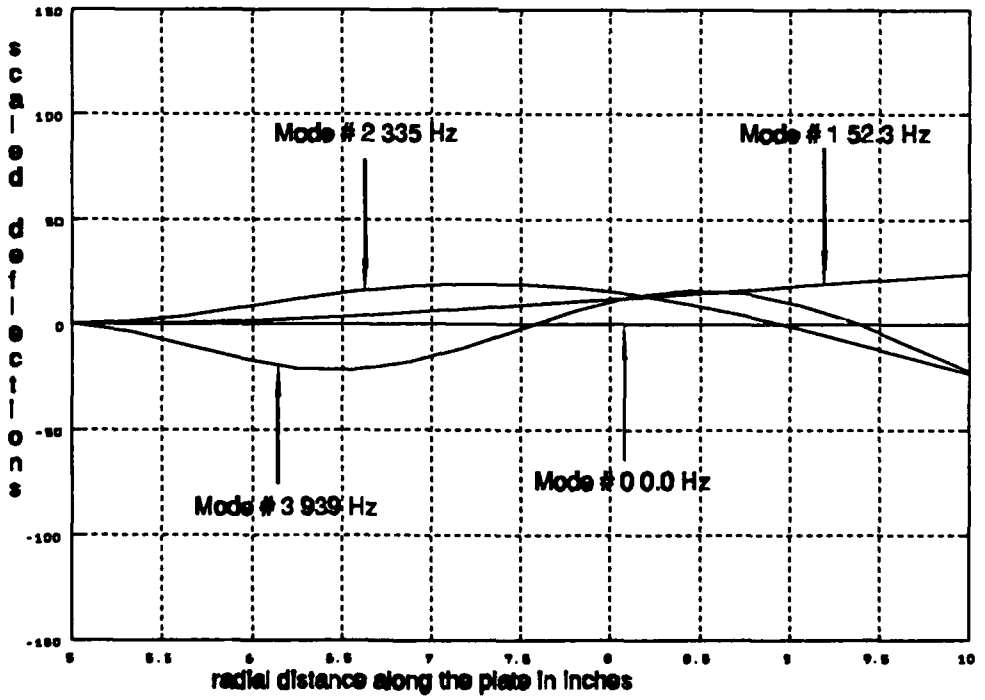

Figure 6. First Three Mode Shapes for Plate

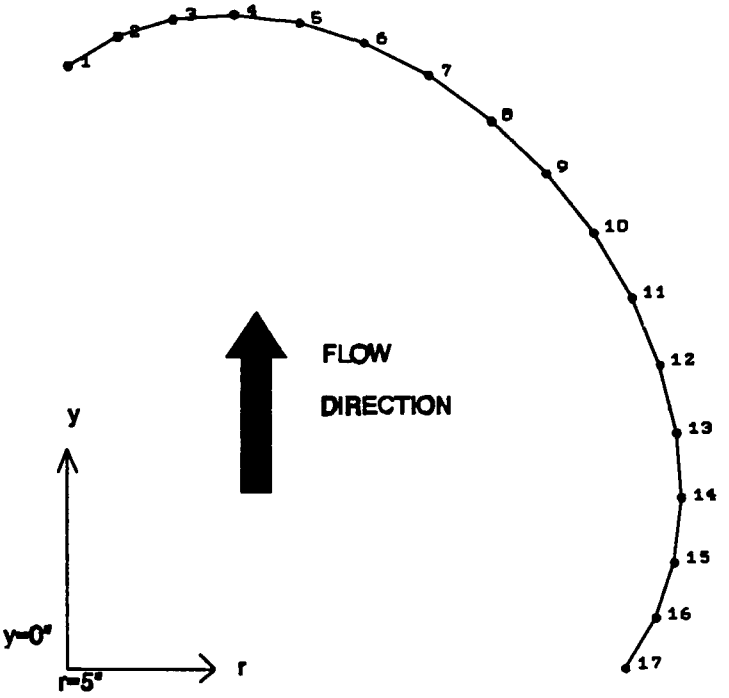

Figure 7. Node Numbers for case 1

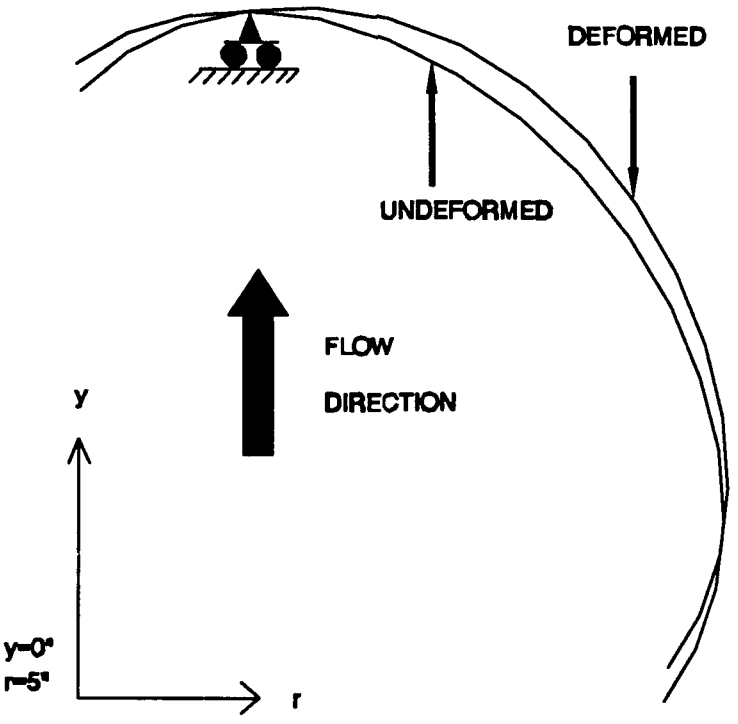

Figure 8. Superposition of deformed and undeformed cross section

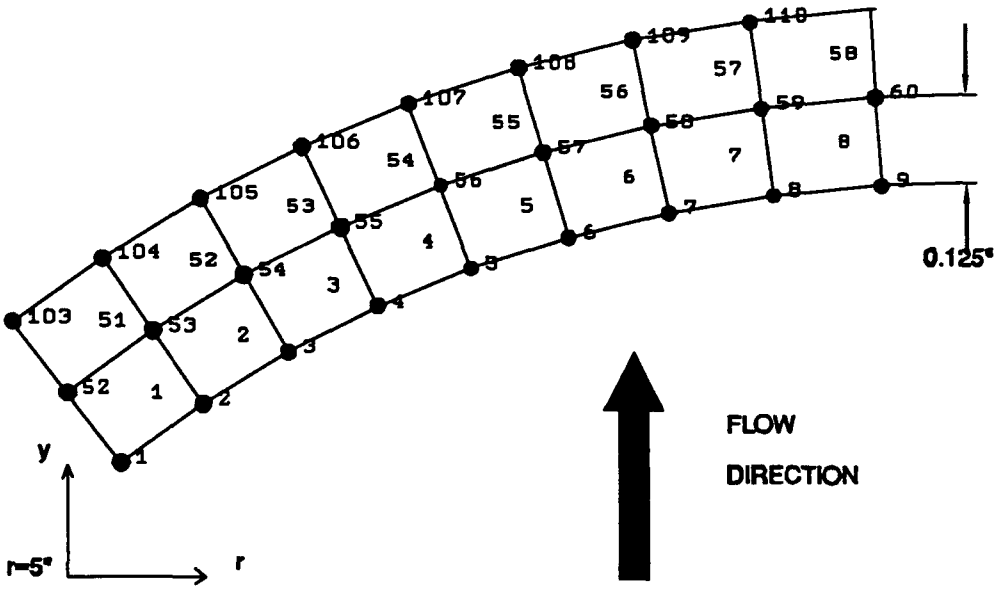

Figure 9. Node and Element numbering for case 3

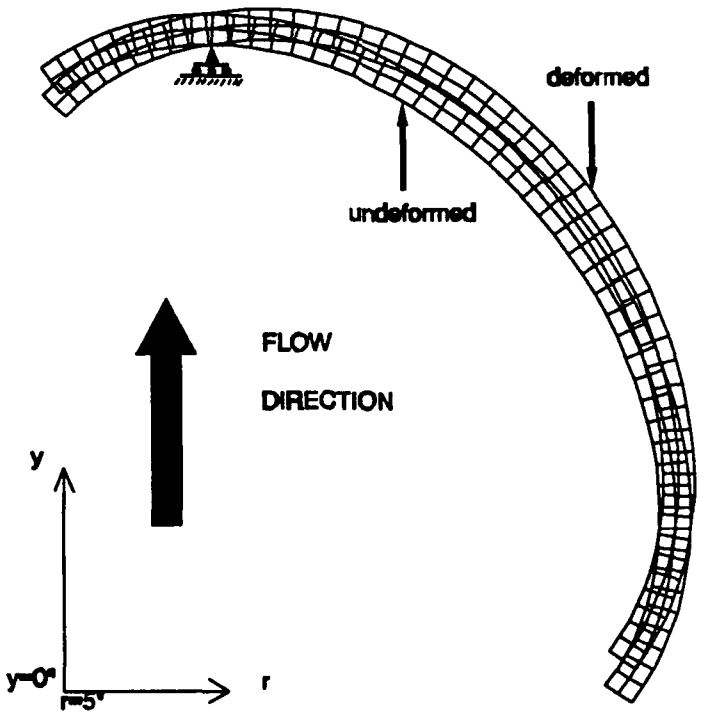

Figure 10. Superposition of deformed and undeformed model case 3

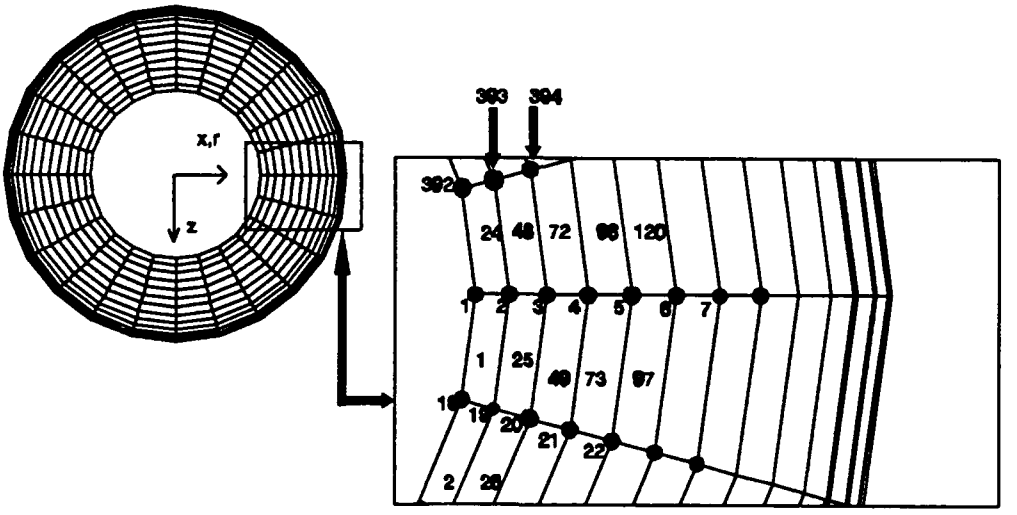

Figure 11. Node and Element Numbering for Case 4 & 5

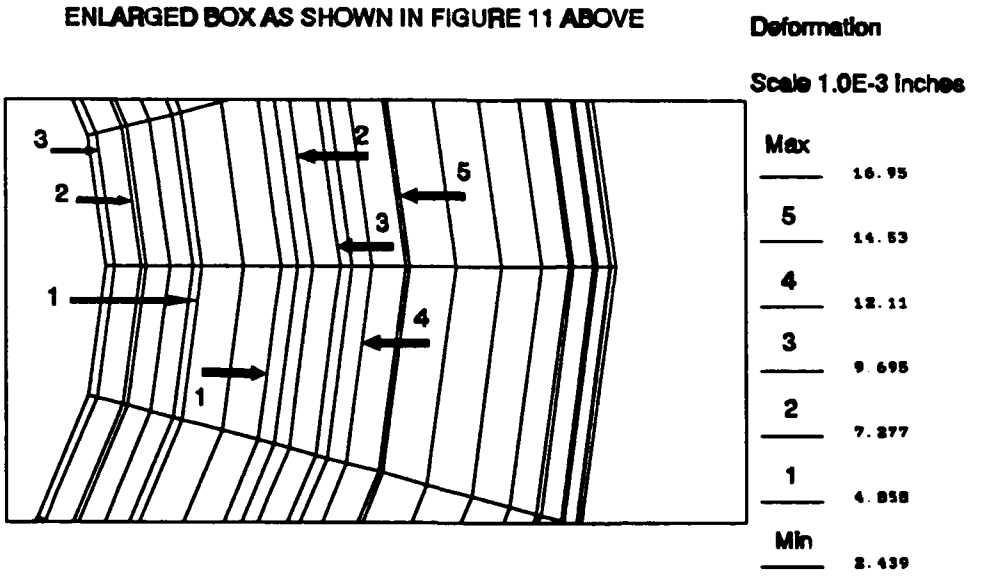

Figure 12. Resultant displacements case 4

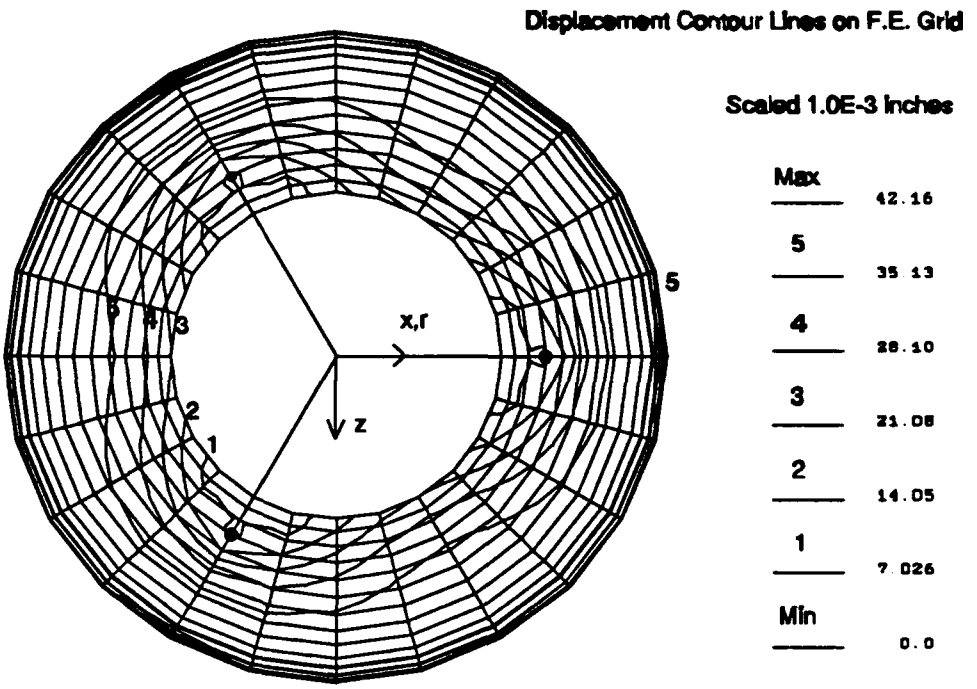

Figure 13. Resultant Displacement Three Point Constraint

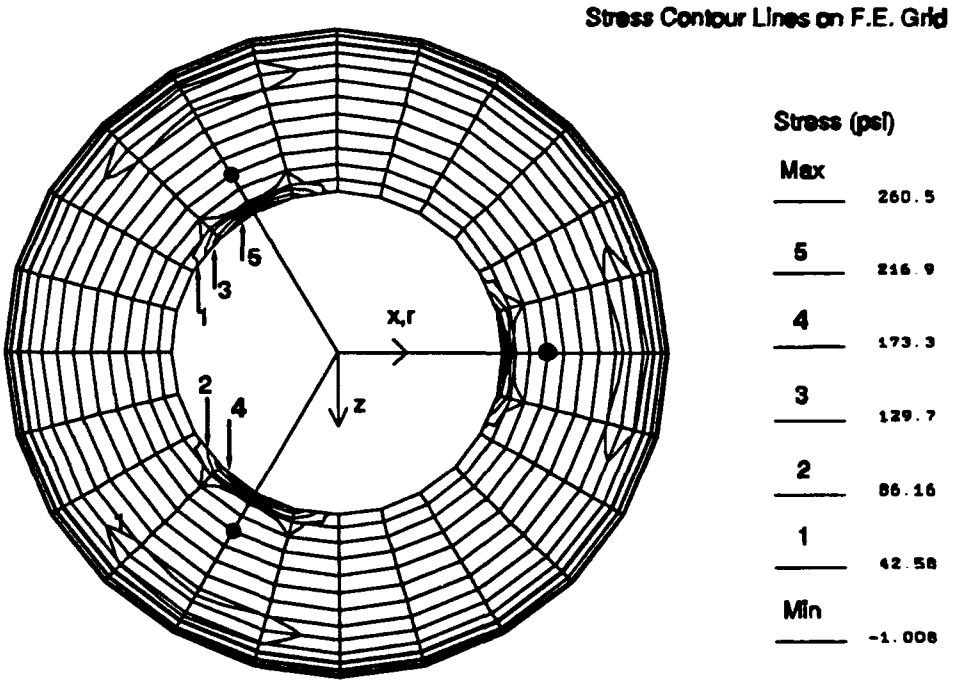

Figure 14. Middle Surface Principal Stress σ_{P1}

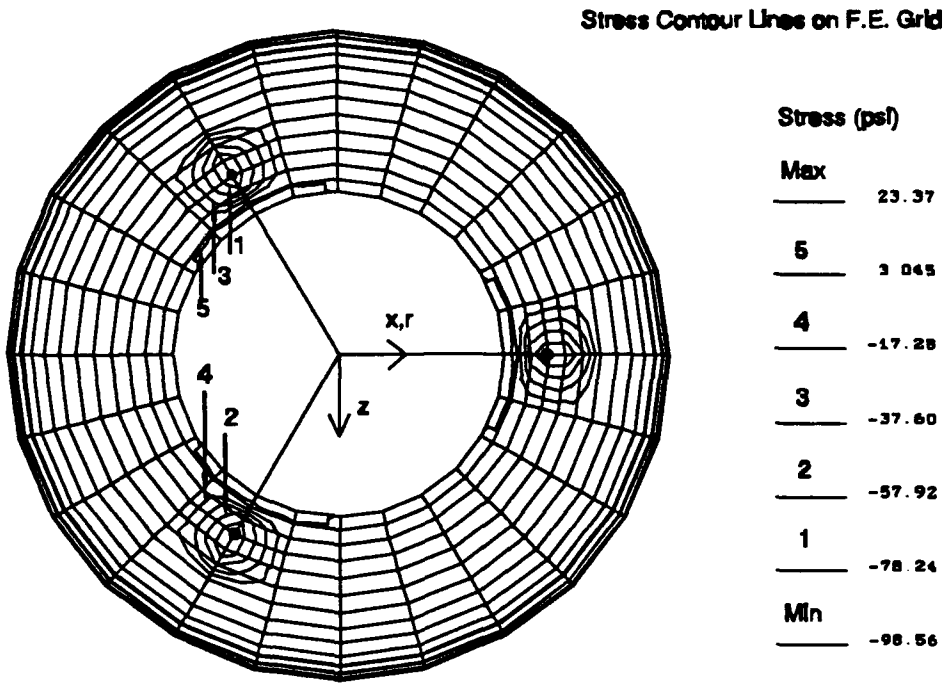

Figure 15. Middle Surface Principal Stress σ_{P2}

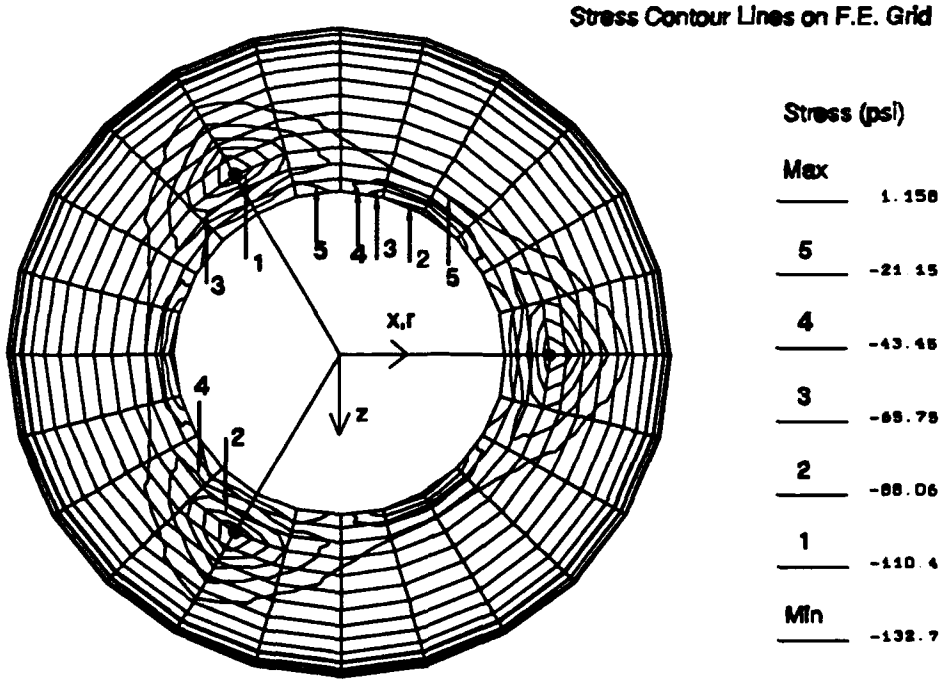

Figure 16. Middle Surface Principal Stress σ_{P3}

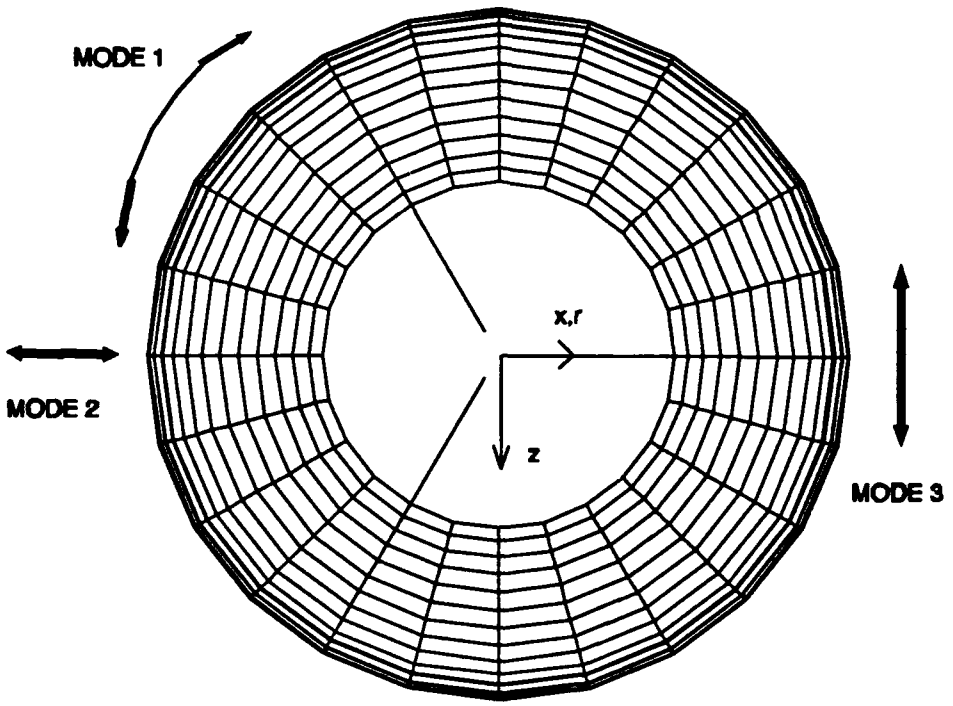

Figure 17. Mode Shapes 1,2, and 3

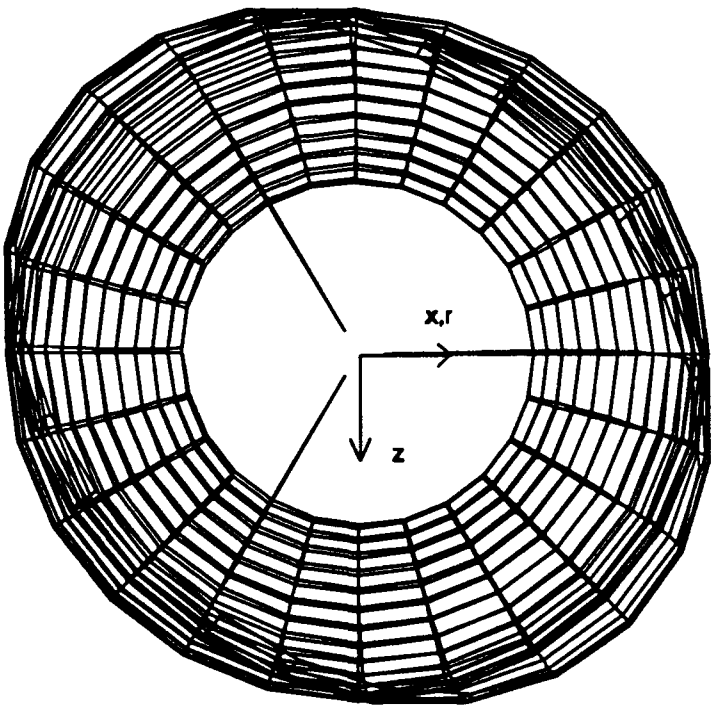

Figure 18. Mode Shapes 4 and 5

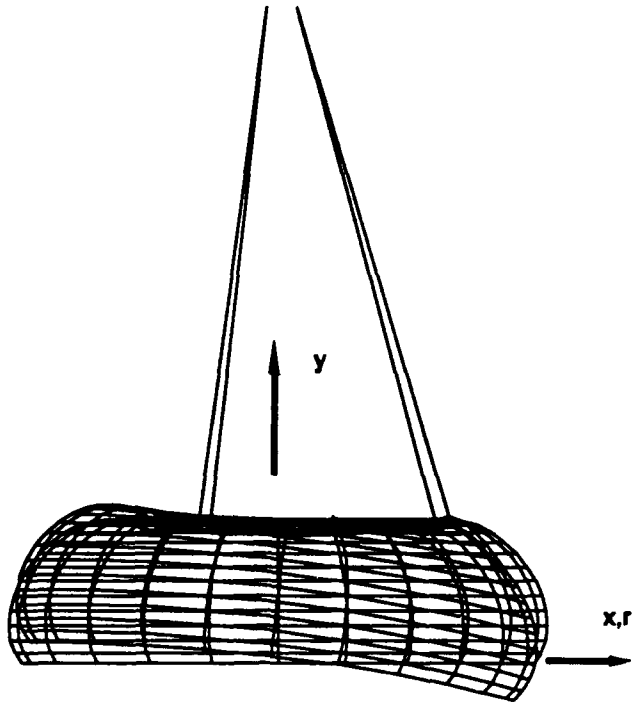

Figure 19. Mode Shapes 6 and 7

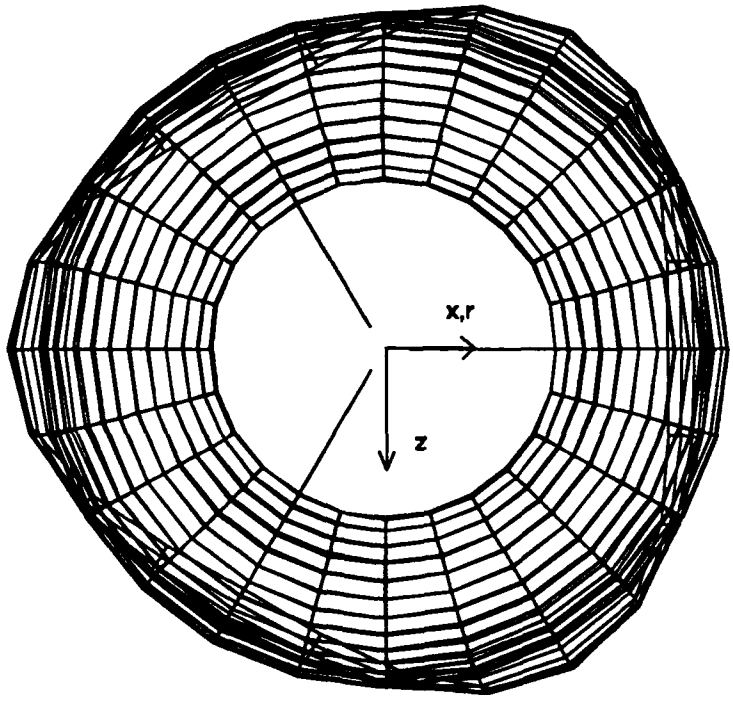

Figure 20. Mode Shapes 8,9, and 10

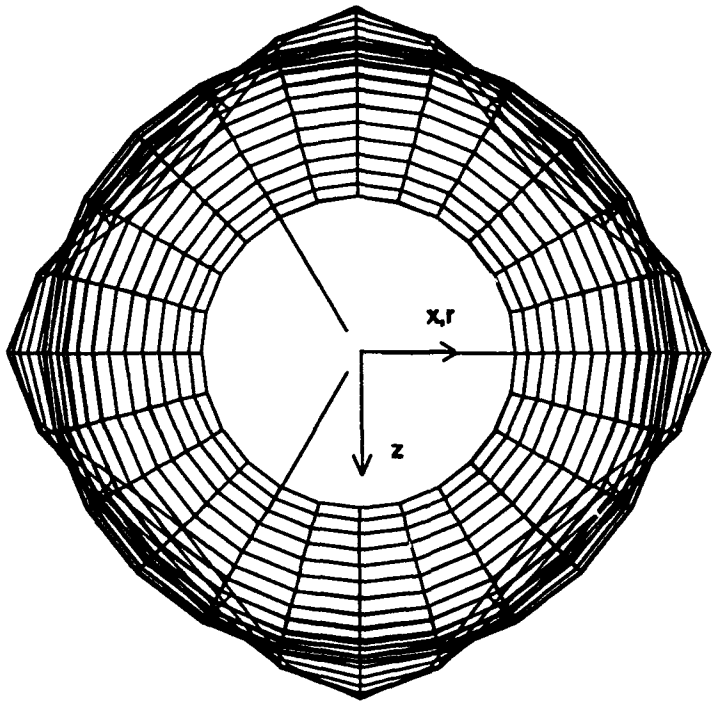

Figure 21. Mode Shapes 11 and 12